ON-GROUND TESTING OF AUTONOMOUS GUIDANCE FOR MULTIPLE SATELLITES IN A CLUSTER

Markus Schlotterer[*], Eviatar Edlerman[†], Federico Fumenti[‡], Pini Gurfil[§], Stephan Theil[¶], Hao Zhang[‖]

The concept of flying multiple satellites in formation has evolved to encompass challenging concepts such as disaggregated space architectures and in-orbit assembly, which include very large numbers of modules flying autonomously in a cluster. Whereas control laws for satellite formations are abundant, guidance and control algorithms for operating large numbers of satellites in close proximity are ongoing research. One approach is to use artificial-potential-based guidance and control laws. This technique uses the definition of several behavior functions like Gather, Avoid and Dock, which form a virtual potential from which desired velocities are computed. A controller is used to achieve these velocities by commanding the onboard thrusters. In a joint research project between the Distributed Space Systems Lab at the Technion and DLR's Institute of Space Systems this approach has been implemented in two different test facilities. Experiments performed in simulation and on the testbeds include formation acquisition and reconfiguration as well as collision avoidance. This paper will present the algorithms as well as the experimental results. They will show the performance and the robustness of the implemented guidance algorithm, as well as the adaptability of the method to different test setups.

INTRODUCTION

These days the size of satellites is limited due to the available shipping volume of modern launch vehicles. To one end, larger and larger structures are needed by future missions to e.g. improve Earth observation capabilities and the resolution of telescopes. These large structures need to be assembled in space. The approach for docking separated these modules to a larger structure is known. However, the research on control of a large number of elements in proximity before assembly remains open. To the other end, modern concepts of disaggregated spacecraft or fractionated spacecraft and sensors require similar loosely constrained flight, clustering the different agents in a defined volume.

For a large number of agents the effort for operation becomes more and more demanding. Thus the introduction of efficient and scalable autonomous methods for guidance and control are needed.

[*]Researcher, GNC Systems Department, German Aerospace Center (DLR)– Institute of Space Systems, Robert-Hooke-Str. 7, 28359 Bremen, Germany
[†]Researcher, Distributed Space Systems Lab, Technion - Israel Institute of Technology, Technion City, Haifa 32000, Israel
[‡]Researcher, GNC Systems Department, German Aerospace Center (DLR)– Institute of Space Systems, Robert-Hooke-Str. 7, 28359 Bremen, Germany
[§]Researcher, Distributed Space Systems Lab, Technion - Israel Institute of Technology, Technion City, Haifa 32000, Israel
[¶]Head of Department, GNC Systems Department, German Aerospace Center (DLR)– Institute of Space Systems, Robert-Hooke-Str. 7, 28359 Bremen, Germany
[‖]Researcher, Distributed Space Systems Lab, Technion - Israel Institute of Technology, Technion City, Haifa 32000, Israel

One approach for solving this problem is the application of artificial potentials to combine different behaviours for each individual spacecraft. Since these algorithms must work autonomously with only a small interaction from operators they need to be extensively tested on-ground.

To test these algorithms different paths could be taken. Numerical simulations - of course - are always the basis for verification. However, the tests with hardware - even with constrained dynamics - help much to understand the effect of uncertainties and errors - inherent to real hardware - on the algorithms. In order to get an understanding on how the tests in on-ground test facilities can be transferred, tests in two different setups are carried out.

One facility is the Test Environment for Applications of Multiple Spacecraft (TEAMS) which has been developed and built by DLR's Institute of Space Systems in Bremen, Germany. The testbed is a laboratory for simulating the force and torque free dynamics of several satellites on ground using air cushion vehicles floating on two big granite tables. It can be used to simulate precise formation flying, as in astronomical missions, and attitude control using 2 vehicles with a rotatable upper platform. 4 smaller vehicles are also available and can be used to simulate swarm behavior, formation acquisition, reorientation and reconfiguration as well as path-planning algorithms. The facility is also useful for testing sensors for relative attitude and position as well as spacecraft behavior during berthing and docking maneuvers (contact dynamics).

Another facility is the Distributed Space Systems Laboratory (DSSL) at Technion, Haifa, which is also a testbed used for testing satellite cluster flight technologies. It uses also an air cushion system to provide friction-less motion in translation and rotation for a small number of vehicles. It also can be used to simulate swarm behavior and formation control.

This paper presents the implementation of an autonomous and distributed path planning algorithm for multiple satellite applications in the two testbeds TEAMS and DSSL. The results are analyzed and compared to simulation results.

The algorithm under test is based on the virtual potential method. It gives the possibility to include different generic behaviors like gathering, docking and avoiding, without the need for precalculation of desired trajectories. From the potentials desired velocities are computed onboard and controlled using a control algorithm.

The path-planning algorithm has not only been implemented in simulation to show its functionality but is also used to guide and control the vehicles on the testbeds. The guidance algorithm is running in real-time on the testbed computers together with a Kalman-Filter for state estimation, attitude control and thruster actuation algorithms. Several experiments have been performed on the testbeds. They include formation acquisition and reconfiguration, as well as collision avoidance. The results of the experiments will show the performance and the robustness of the implemented guidance algorithm on the two testbeds TEAMS and DSSL.

PATH-PLANNING AND CONTROL

The path-planning approach used in this paper has been proposed by Izzo and Pettazzi.[1] It is based on the definition of a virtual potential field from which desired velocities $\underline{v}_d$ can be derived. These desired velocities are a sum of different weighted contributions named "behaviors". To track the desired velocity different control methods can be used. The derivation of equations and simulations of this approach were presented by Schlotterer et. al.[2] The definitons of the kinematical field as well as the control design approach are repeated here for sake of completeness.

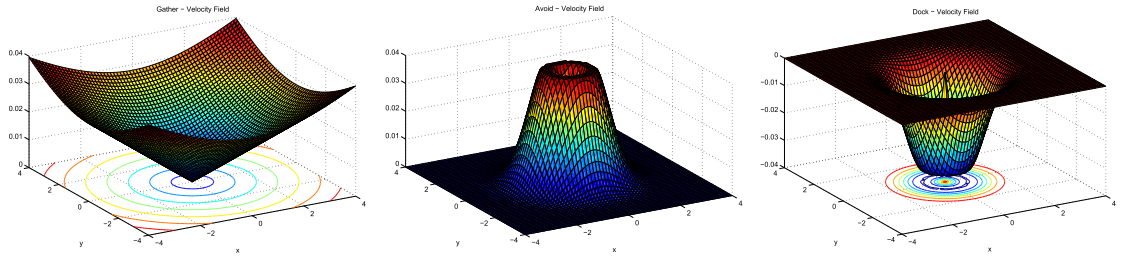

(a) Gather behavior (b) Avoid behavior (c) Dock behavior

Figure 1. Agent behaviors

Definition of the kinematical field

Consider N spacecraft (agents) with their position $\underline{x}_i$ in the local horizontal local vertical (LHLV) reference frame and the same number of target points at position $\underline{\xi}_j$. To steer these agents to their target positions 3 different behaviors are introduced.

The *Gather* behavior makes the agents move in the direction of the targets:

$$\underline{v}_i^{Gather} = \sum_j c_i \left(\underline{\xi}_j - \underline{x}_i \right) \tag{1}$$

with positive constants c_i defining the intensity of the attraction. The desired velocity is proportional to the distance and as such globally effective (see Fig. 1(a)).

The *Avoid* behavior defines an interaction between different spacecraft. In case that these spacecraft are in proximity to each other a repulsive component is added to the kinematical field:

$$\underline{v}_i^{Avoid} = \sum_j -b_i \exp\left(-\frac{\left\| \underline{x}_j - \underline{x}_i \right\|^2}{k_{a,i}} \right) \left(\underline{x}_j - \underline{x}_i \right) \tag{2}$$

with the positive constants b_i, which defines the intensity, and $k_{a,i}$, which defines the sphere of influence (see Fig. 1(b)).

Finally, the *Dock* behavior defines local attractors towards the target points (see Fig. 1(c)). This behavior has only a nonnegligible value in the vicinity of the target points. Again, a constant d_i is defined for the intensity and a constant $k_{d,i}$ for the sphere of influence:

$$\underline{v}_i^{Dock} = \sum_j d_i \exp\left(-\frac{\left\| \underline{\xi}_j - \underline{x}_i \right\|^2}{k_{d,i}} \right) \left(\underline{\xi}_j - \underline{x}_i \right). \tag{3}$$

The total desired velocity for each spacecraft $\underline{v}_i$ is the sum of these three components:

$$\underline{v}_i = \underline{v}_i^{Gather} + \underline{v}_i^{Avoid} + \underline{v}_i^{Dock}. \tag{4}$$

Assuming a symmetric formation configuration, the parameter vector $\underline{\lambda}_i = [b_i, c_i, d_i, k_{a,i}, k_{d,i}]$ will be the same for each spacecraft. The parameter vector $\underline{\lambda}$ has to be chosen such that the final configuration is an equilibrium point (*Equilibrium Shaping*). That means that the desired velocity must

be zero when the agents have reached their final position:

$$\underline{v}_i \left(\underline{x}, \underline{\xi}, \underline{\lambda} \right) \Big|_{\underline{x}=\underline{\xi}} = 0. \tag{5}$$

This results in a system of equations which can be solved for one parameter if the others are given.

Control methods

The kinematical field computes desired velocities. To reach these velocities each vehicle needs a controller to produce the needed thrust. In[1] three different control methods have been proposed: "Q-Guidance", "Sliding-Mode Control" and "Artificial Potential". Novoschilov et. al.[3] compared these three methods to each other and selected the "Artificial Potential" approach for further simulations and experiments on a testbed.

The feedback control law can be obtained from the virtual potential function given by

$$V = \frac{1}{2} \sum_i \underline{v}_i \underline{v}_i + \sum_i \sum_{j \neq i} \phi_A^{ij} \left(\underline{x}_i - \underline{x}_j \right) + \sum_i \sum_j \phi_G^{ij} \left(\underline{x}_i - \underline{\xi}_j \right) + \sum_i \sum_j \phi_D^{ij} \left(\underline{x}_i - \underline{\xi}_j \right) \tag{6}$$

with

$$\frac{\partial \phi_A^{ij}}{\partial \underline{x}_i} = -\underline{v}_i^{Avoid} \qquad \frac{\partial \phi_G^{ij}}{\partial \underline{x}_i} = -\underline{v}_i^{Gather} \qquad \frac{\partial \phi_D^{ij}}{\partial \underline{x}_i} = -\underline{v}_i^{Dock}. \tag{7}$$

This function has equilibrium points for each combination of agents at the target points $\underline{\xi}_i$. According to Lyapunov's theorem the system will reach its equilibrium point if

$$\dot{V} = \sum_i \left(\frac{\partial V}{\partial \underline{x}_i} \dot{\underline{x}}_i + \frac{\partial V}{\partial \underline{v}_i} \dot{\underline{v}}_i \right) = \sum_i \left(\dot{\underline{v}}_i - \underline{v}_{d_i} \right) \underline{v}_i < 0. \tag{8}$$

Using the feedback law

$$\underline{u}_i = \underline{v}_{d_i} - \kappa_i \underline{v}_i - \underline{a}_{in_i}, \tag{9}$$

in which $\underline{a}_{in_i}$ is the natural differential acceleration between reference point and satellite, the time derivative of the potential function is

$$\dot{V} = \sum_i \underline{v}_i \left(-\kappa_i \underline{v}_i + \underline{a}_{dis} \right) \tag{10}$$

with the acceleration due to non-modeled disturbance forces $\underline{a}_{dis}$. This can be made negative as long as the lower bound $\kappa_i > \frac{\|\underline{a}_{dis}\|}{\|\underline{v}_i\|}$ is applied.

ON-GROUND TEST FACILITIES FOR SATELLITE FORMATION FLYING AND CLUSTER FLIGHT

For testing the formation and cluster control based on artificial potentials in a representative hardware environment two different test setups are used. Before discussing the limitations and characteristics of tests in these facilities, both are introduced in the following sections.

The TEAMS facility

For the on-ground validation of the path-planning and control algorithms the TEAMS (Test Environment for Applications of Multiple Spacecraft) facility at the Institute of Space Systems of the German Aerospace Center in Bremen has been used.

TEAMS is a laboratory to emulate the force and torque free dynamics of satellites on ground. It consists of two granite tables with a total experiment area of 5 m by 4 m (see Fig. 2). The surface of each table has been manufactured with an accuracy of 3 µm. In addition the tables have been leveled with an accuracy of less than 20 µm from one edge to the other and with an accuracy of less than 10 µm from one table to the other.

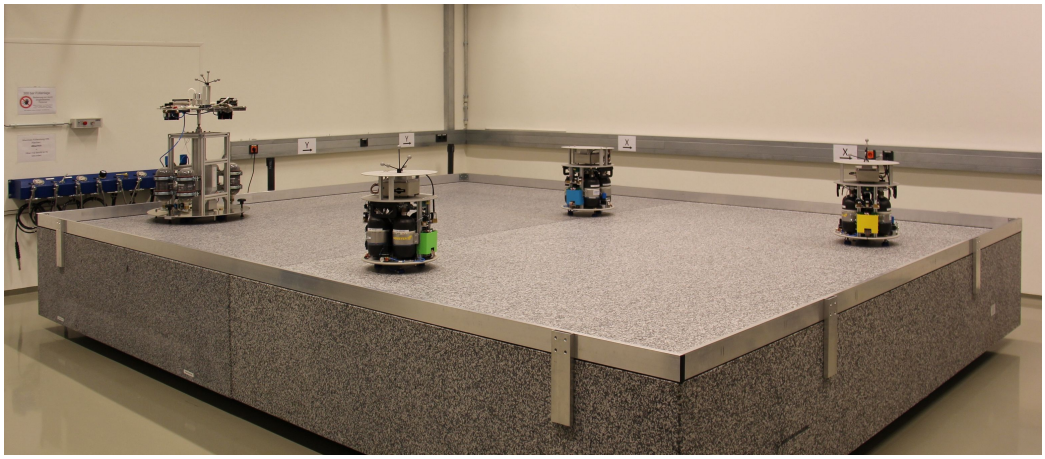

Figure 2. TEAMS laboratory

Spacecraft are represented by air cushion vehicles. Two types of air cushion vehicles are used: The 2 bigger ones called TEAMS_5D have an actuated linear stage to simulate movement in the z-axis and will have a rotatable upper platform to simulate attitude dynamics ("Attitude Platform"). These vehicles can emulate 5 degrees of freedom (see Fig. 3(a)). The 4 smaller vehicles are called TEAMS_3D and are able to emulate 3 degrees of freedom (Fig. 3(b)). These are used mainly for swarm simulations.

Beneath each vehicle three air cushion pads generate a small air film on which the vehicles can float frictionless. The air for the air bearings as well as for the thrusters is stored in several 300 bar air tanks. Pressure regulators regulate the air pressure down to 6–8 bar. On the TEAMS_5D vehicles a spherical air bearing supports the rotatable upper platform.

A *DTrack* infrared tracking system is used as main sensor for position and attitude. Several reflective balls are mounted on each vehicle and are tracked by 6 infrared cameras. By combining the images of these cameras the tracking system can compute position and attitude of each vehicle. As the configuration of the reflective balls is different for each vehicle the system is able to distinguish between the agents. The position and attitude of each vehicle is distributed over the local wireless network and can be used by each onboard computer. In addition the TEAMS_5D vehicles will also use an inertial measurement unit with three fiber optic gyros and three MEMS accelerometers.

To control position and attitude the vehicles are equipped with proportional coldgas thrusters supported by 6 bar pressurized air. The TEAMS_5D thrusters can produce a maximum thrust of

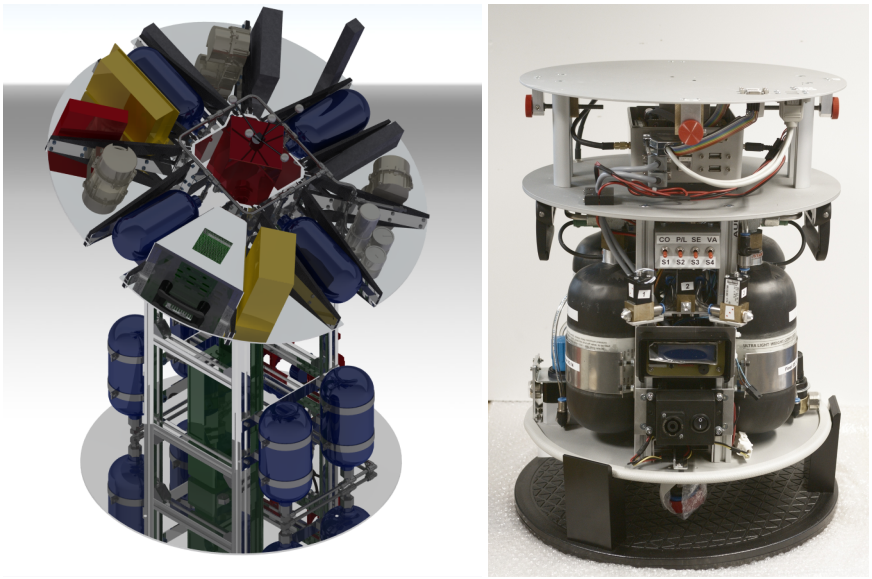

(a) TEAMS_5D (b) TEAMS_3D

Figure 3. TEAMS air cushion vehicles

65 mN while the maximum thrust of the TEAMS_3D thrusters is 47 mN. Depending on thruster configuration and vehicle mass the thruster system can produce an acceleration of 2.8 mm/s^2 (TEAMS_5D, current configuration) and 5.5 mm/s^2 (TEAMS_3D). In addition the attitude platform of the TEAMS_5D vehicles will be equipped with 3 reaction wheels with a maximum commandable torque of 0.015 Nm and a maximum angular momentum of 0.36 Nms. As these wheels are only for attitude control they are not used in the experiments described in this paper.

As onboard computer an embedded x86 Atom Z530 on a PC104 stack is used running the *QNX* RTOS. Via a WLAN connection software and parameters can be uploaded and realtime data can be downloaded, displayed or saved. Control algorithms are developed using *Matlab/Simulink* together with *Real-Time Workshop* (RTW) for automatic generation of C-code.

Beside the described control and path-planning algorithms a Kalman-Filter for state estimation, a thruster actuation (TA) algorithm as well as algorithms for attitude control are running on the onboard computer. The Kalman-Filter is a static gain filter for estimation of velocities, attitude rate, constant disturbing acceleration and constant disturbing angular acceleration. The TA algorithm is needed to compute the needed thrust of each thruster given the thruster configuration and the commanded forces and torques. Attitude control around the z-axis is implemented as a LQR with static disturbance rejection using the outputs of the Kalman-Filter (see[4]).

The DSSL facility

The Distributed Space Systems Laboratory (DSSL) at Technion, Haifa, is a unique testbed used for testing satellite cluster flight technologies. Fig. 4 describes a general layout of the DSSL experimental facilities, which include an air table, a ground station, robots and a communication system.

The 3.5×3.5m air table, shown in Fig. 5 provides a uniform flow field by enabling throughput of compressed air.

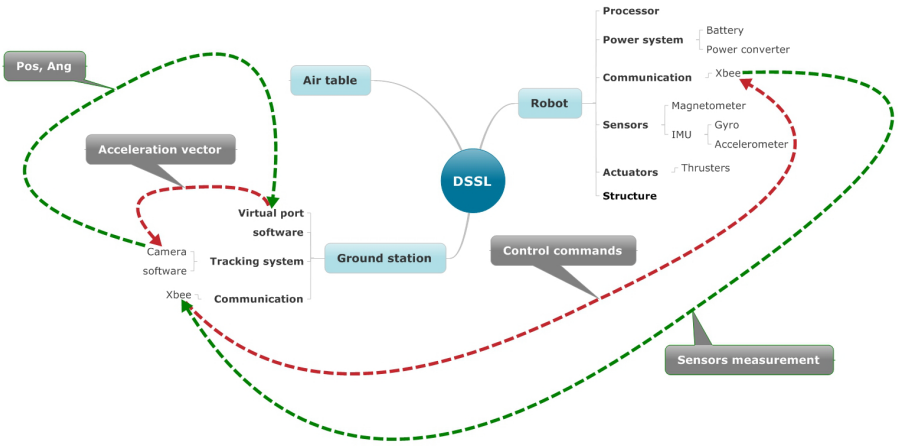

Figure 4. General layout of DSSL

Figure 5. The air table in DSSL

The robots were produced using a 3D printer, and are made of ABS plastic. Figure 6 shows the robot configuration, which includes a 3mm thick glass plate used for floatation. With a diameter of 300mm, the plate creates enough floatation force to reduce the friction. The lower part of the robot includes the battery and thrusters, while the upper part includes the required electronics.

The robots' on board magnetometer is used for measuring orientation. The magnetometer uses the Earth magnetic field reference to find the magnetic north. The magnetometer is noisy and may be affected by magnets, metals and electromagnetic fields, and therefore a calibration procedure is used. The inertial measurement unit (IMU) includes a rate gyro and accelerometers. In Fig. 7, the

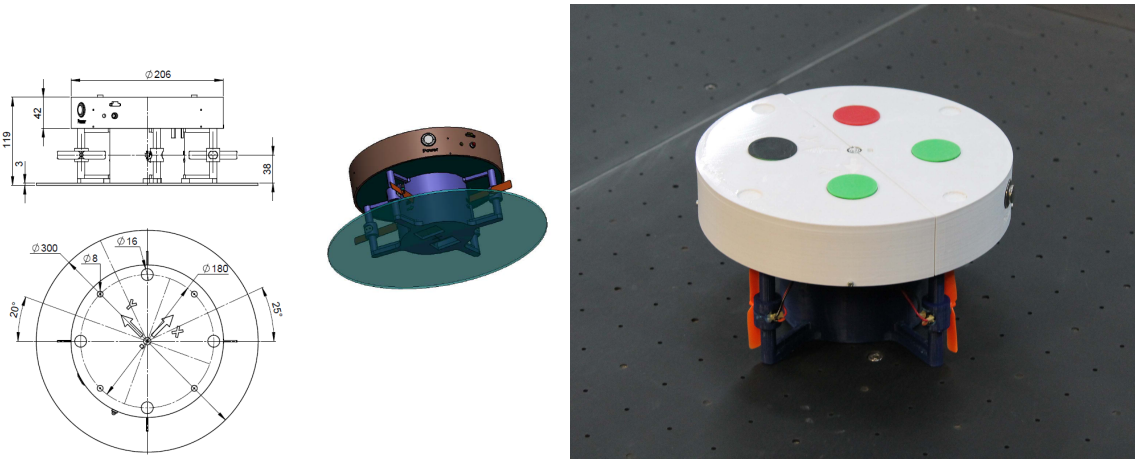

(a) Mechanical layout (b) Current configuration

Figure 6. The robots used in DSSL for cluster flight experiments

main electronic board of the robot, which includes the IMU, is shown.

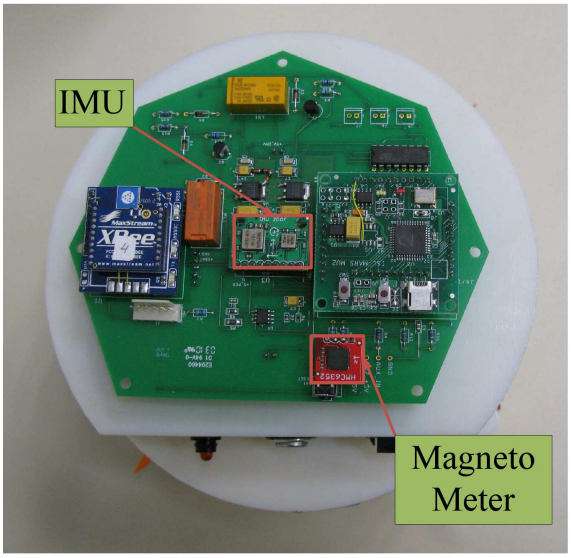

Figure 7. Robot's electronic board

The robots' actuation forces are applied by four thrusters, with each one applying force in one direction only (see Figure 8). The thrusters are located within a fixed distance from the center of mass and therefore create both force and torque. The system works with the thrusters in an on/off mode. The thrusters performance is listed in Table 1. A Lithium-Polymer rechargeable battery provides the power needed for the thrusters and the electronics.

The thruster controller produces a continuous commanded state whereas the motor can only work in a on/off mode. Therefore, it is necessary to transform the continuous command to an on/off signal. One way to solve this problem is to use a bang-bang controller. The bang-bang controller is simple for implementation, but it uses a considerable control effort. Another option is to use

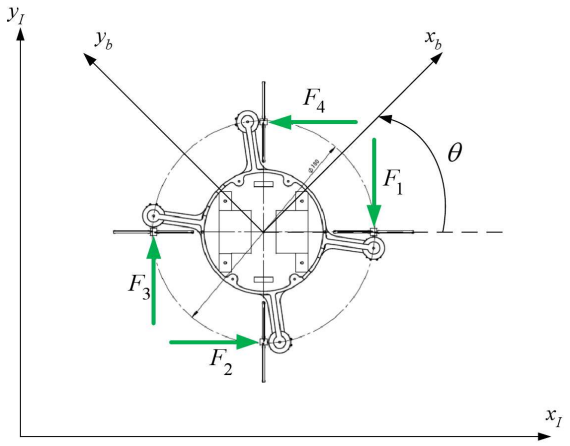

Figure 8. Forces applied by the thrusters

Voltage (v)	Current (A)	Thrust (g)	Power (w)	Efficiency (g/w)
6.0	0.52	17.24	3.14	5.49
7.2	0.69	22.41	4.94	4.53

Table 1. Thruster performance

pulse modulators. One well-known method is pulse-width modulation (PWM), in which the output pulse width is proportional to the level of the continuous control command. PWM requires a high frequency when using electric motors. In the current system pulse-width pulse-frequency (PWPF)[5,6,7] was implemented. The PWPF creates an output pulse width which is proportional to the level of the continuous control command, but also changes the pulse frequency. With the low rate communication frequency in the lab, the feature of controlling the pulse frequency is crucial.

The PWPF consists of a first order filter, a Schmitt-trigger (a bistable circuit in which the output increases to a steady maximum when the input rises above a certain threshold, and decreases almost to zero when the input voltage falls below another threshold) and a unit feedback. The PWPF yields a quasi-linear, accurate and adjustable thruster operation.

The communication system between the robots and the ground station is based on Xbee devices. An overhead tracking system provides reference measurements of position and orientation. The tracking software consists of image processing, detection, and measurement modules, managed by a graphical user interface as shown in Fig. 9). The tracking software detects the color patterns on the robots, calculates the center of mass of the patterns, thereby providing the robot position. The black circle is used as a reference for attitude calculations.

ALGORITHM VERIFICATION ON GROUND-BASED TESTBEDS

Preliminary Considerations

The application of the artificial potential to formation flying considering orbital dynamics is outlined by Izzo and Pettazzi in[1] and Schlotterer in.[2] The latter was presenting simulations for formation acquisition and control using this approach. The paper showed already results from on-ground experiments.

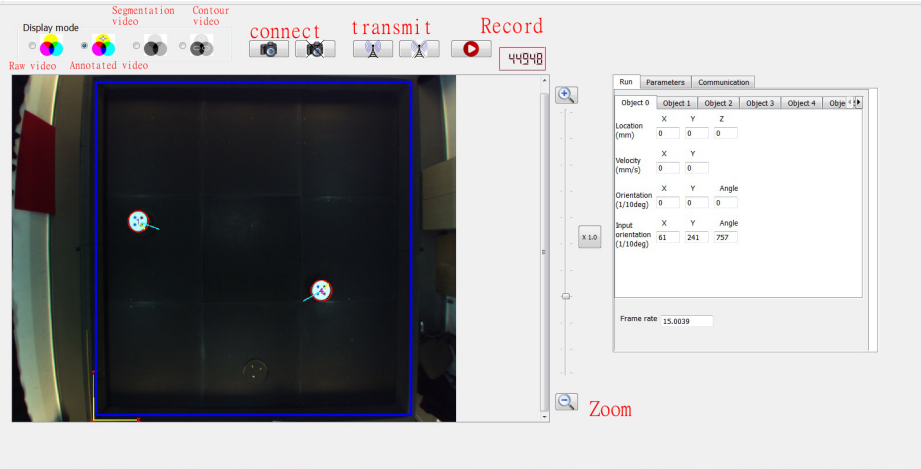

Figure 9. Tracking system GUI

When algorithms - here the control based on artificial potential functions - are tested in on-ground test facilities then the limitations of the ground-based test setups have to be taken into account. The real 3D problem is transferred to a 2D (planar) problem. Furthermore gravitation and orbital mechanics governing the relative motion of satellites in space are not present in the ground based test facilities. Both factors show that the verification on the test beds cannot be a proof of performance and stability for a later in-orbit application.

However, the testbeds offer to use the algorithms in a real hardware system with different but still representative dynamics. With application to a real hardware system the verification on the testbed allows to check the algorithm's robustness against typical expected but also unexpected deviations. The experience and the results from these kind of experiments are invaluable since they allow to see the impact of a real environment at an early development stage. Although the driving gravity force is not present the dynamics resembles the basics of relative motion and the order of the controlled dynamics is similar.

Depending on the algorithm to be tested the value of the test is different. For a navigation sensor or algorithm the general functionality can be verified. In case the navigation algorithm is independent from the dynamics model the test results would be fully representative. For a control the transferability of results is probably lowest since the controller is always fit to the system setup. Therefore only the general control design approach could be verified. When testing a guidance function it depends whether it exploits natural driving forces inherent to the controlled dynamics. As soon as the guidance function becomes more abstract and independent from the dynamics the testbeds can provide a very useful environment for verification. This is applicable to the artificial potential approach. The kinematic field provides the desired velocities this is independent from the dynamics and only based on the actual positions and velocities. Then the controller creates the needed actuation commands to achieve the required velocities and considers the dynamics of the system. Thus the artificial potential approach guidance function is an excellent example for representative tests in a ground based test facility.

With this setup, robustness and functionality of the guidance function can be demonstrated. This provides many lessons learned which could be very costly in space in case of errors. If there is an option to test the same algorithm in two different test facilities, a strategy can be developed enabling

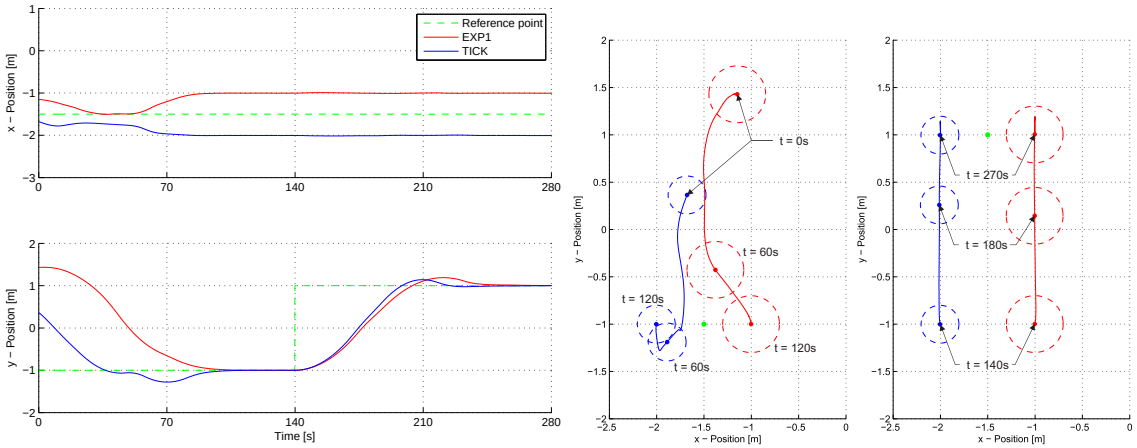

(a) Formation acquisition and repositioning (b) Formation acquisition (c) Formation repositioning

Figure 10. Formation acquisition and repositioning for a fixed target

an easier transfer of algorithms into different setups which in turn helps to transfer algorithms to space applications.

Results on TEAMS facility

The experiments presented in the following section has been made using the currently available TEAMS_5D vehicle called "Exp1" and one TEAMS_3D vehicle called "Tick". The size of the sphere of influence for the *Avoid* and *Dock* behavior have been chosen to $k_a = k_d = (0.5\,\mathrm{m})^2$. The maximum velocity $v_{max} = 0.07\,\mathrm{m/s}$ has been set such that the vehicles can decelerate within one meter. This results in the choice of the parameters $b = 1.2\,\mathrm{s}^{-1}$ and $d = 0.1\,\mathrm{s}^{-1}$. Using the *Equilibrium Shaping* method the last parameter can be computed to $c = 0.0102\,\mathrm{s}^{-1}$.

Formation acquisition The experiment presented in this section includes a formation acquisition as well as a formation reconfiguration. At the beginning of the experiment the vehicles are placed randomly on the table. The target points are defined to $\underline{\xi}_1 = [-1\,\mathrm{m}, -1\,\mathrm{m}]$ and $\underline{\xi}_2 = [-2\,\mathrm{m}, -1\,\mathrm{m}]$. The results are shown in Fig. 10(a) and Fig. 10(b).

At the beginning both vehicles orient themselves in the direction of the formation center. At this point the kinematical field is mainly influenced by the *Gather* behavior. The smaller "Tick" vehicle is the first to arrive at the reference y-value and waits near its final position for the arrival of the "Exp1" vehicle. The bigger "Exp1" vehicle then pushes the "Tick" vehicle into its final target position. The acquisition time for the total formation is about 100 s and the residual control error is below 5 mm.

At $t = 140\,\mathrm{s}$ the formation has been reconfigured and new reference points were given. Both vehicle drift to their new target points in an almost parallel way. The acquisition time for this maneuver is about 110 s.

Acquisition of a rotating formation A second experiment demonstrates the acquisition of a rotating formation. The parameters for the kinematical field are the same as in the previous experiment but the target points are rotating on opposite positions around the reference point with $\omega = 0.03\,\mathrm{rad/s}$ on a circle with radius $r = 0.5\,\mathrm{m}$. At the beginning of the experiment the vehicles have been placed randomly on the table. The results are shown in Fig. 11.

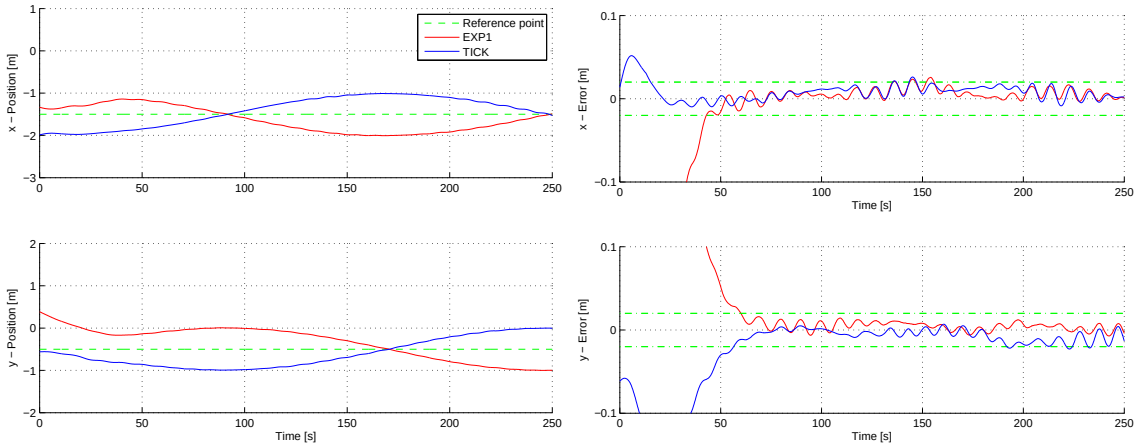

(a) Vehicle position (b) Control error

Figure 11. Acquisition of a rotating formation

The vehicles reach their target points successfully after 61 s. Looking in the details of the control error one can see an oscillation of both vehicles in x as well as in y direction. The reason for this is that the *Avoid* behavior has a strong influence even when both vehicles have reached their target position. The nonlinear feedback from position to desired velocity (Eq. 2) leads to a limit cycle of a nonlinear system of second order. Lowering the strength of the kinematical field would also lower the amplitude of the limit cycle but would also increase acquisition time. Another possible solution for this problem is to reduce the sphere of influence of the *Avoid* behavior which will lower the influence of the *Avoid* behavior on a neighbor vehicle when in final configuration. Again this would lower the amplitude of the limit cycle. The best solution is to adapt the *Avoid* behavior such that there is no influence on other vehicles when outside the sphere of influence.

Collision avoidance The last experiment shows the collision avoidance capabilities of the presented path-planning algorithm. For that a formation consisting of three vehicles forming an equilateral triangle is used. Again, the vehicles "Tick" and "Exp1" are used. The third agent is not a real vehicle but a target of the tracking system, which can be moved manually. But for the other vehicles it is seen as a third agent. As a different formation configuration is used, the parameters for the kinematical field have to be recalculated. They are set to $k_a = k_d = 0.2\,\mathrm{m}^2$, $b = 0.7\,\mathrm{s}^{-1}$, $d = 0.1\,\mathrm{s}^{-1}$ and $c = 0.0141\,\mathrm{s}^{-1}$.

Between $t = 0\,\mathrm{s}$ and $t = 30\,\mathrm{s}$ the formation is in equilibrium state in its final configuration (see Fig. 12(a)). At $t = 30\,\mathrm{s}$ the target of the tracking system is moved according to the trajectory in Fig. 12(a). This simulates an abnormal behavior of one satellite. The "Tick" as well as the "Exp1" vehicle start to move away to avoid a collision with the third agent. As the third agent is not at a target point, both other agents don't move to a target point neither.

Putting the tracking target in the target point $\underline{\xi}_2$ at $t = 91\,\mathrm{s}$ the two vehicles start to rebuild the desired formation automatically and move to the other target points $\underline{\xi}_1$ and $\underline{\xi}_3$.

Results on DSSL facility

This section presents a series of experiments conducted on the DSSL facility. These experiments are similar to those performed on the TEAMS facility. Whereas the experiments are similar, the

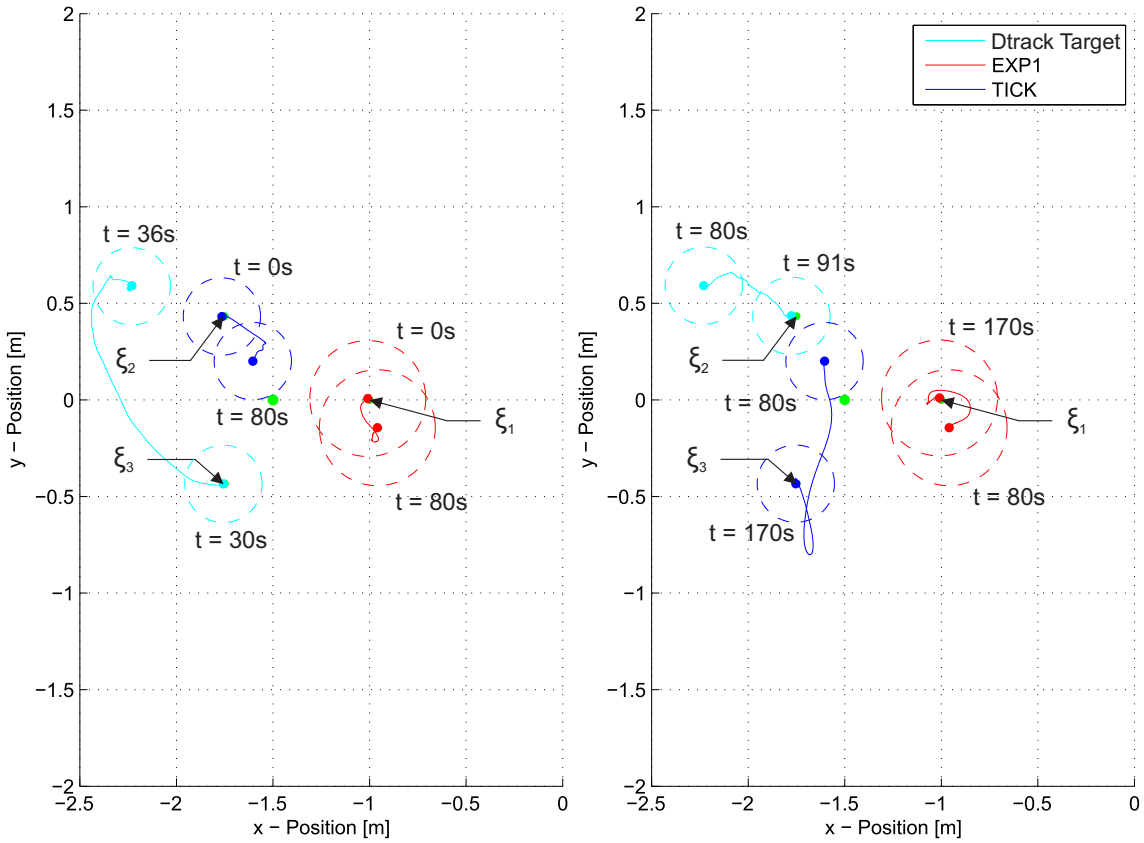

(a) Collision avoidance during abnormal vehicle behavior

(b) Autonomous reconfiguration

Figure 12. Collision avoidance and autonomous reconfiguration

testbeds have some major differences, as discussed in previous sections. Repeating the experiments on different testbeds and different robots obviously increases the reliability and versatility of the guidance and control algorithms.

Three experiments are presented in this section:

1. Formation establishment and reconfiguration
2. Acquisition of a rotating formation
3. Collision avoidance

The parameters for the kinematical field are the same throughout all the experiments,

$$b = 4\,\mathrm{s}^{-1},\ d = 1\,\mathrm{s}^{-1},\ k_a = k_d = 0.4\,\mathrm{m}^2,\ \kappa = 5 \tag{11}$$

The experiment included 3 robots. Initially, the robots are placed randomly on the air table described in the previous section.

Formation establishment and reconfiguration At the beginning of the experiment each robot is moving towards a target position (see Figure 13(c), solid lines). The establishment maneuver takes about 20 s. the target positions are located on a circle with 1.2 m radius (see Figure 13(a)). The target positions are equally divided along the circle so the aspect angle is 120 deg (see Figure 13(b)). After the establishment phase the angular separation is maintained throughout the experiment. Once the robots reach the goals, they maintain their position while maintaining a balance between all the different behaviors dictated by the artificial potential. After 62 s the nominal radius is changed to 0.7 m. The transition maneuver is short and within 10 s the robots reach their new target positions. Due to the thrust to mass ratio (mass less than 1 kg, maximum thrust of 180 mN) the transition maneuvers are fast. Additional transitions happened after 103 s and 152 s. In both cases the transition maneuvers lasted for about 10 s. Another experiment was conducted in a similar manner to confirm the results (see Figure 14).

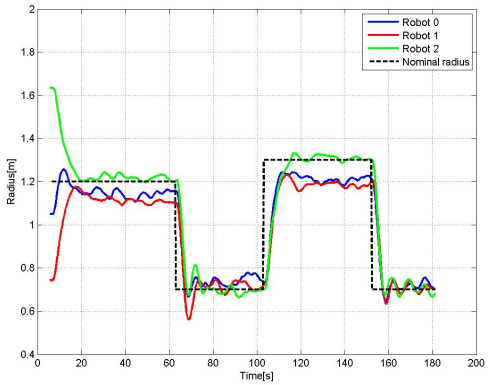

(a) Radius

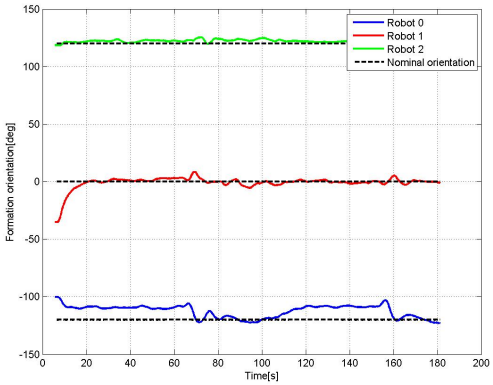

(b) Angular separation

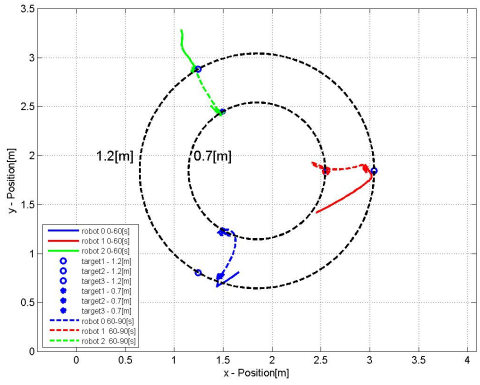

(c) Trajectory

Figure 13. Formation establishment and reconfiguration - experiment 1

Acquisition of a rotating formation The second goal of the experiment is to demonstrate the acquisition of a rotating formation. The first part of the experiment is the same as the establishment experiment (see Figure 15(c), solid lines). Once the robots reach their target positions, the target positions start to rotate with an angular velocity of $\omega = 0.043$ rad/s on a circle with a radius $r =$

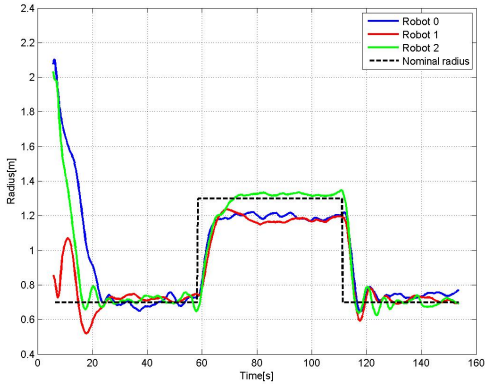

(a) Radius

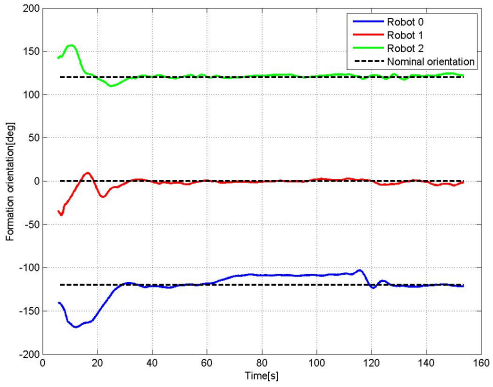

(b) Angular separation

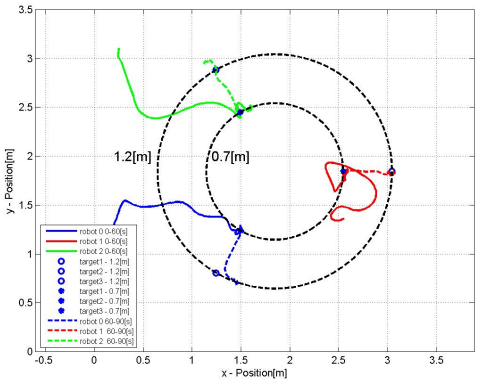

(c) Trajectory

Figure 14. Formation establishment and reconfiguration - experiment 2

1.3 m. The results are depicted in Figure 15. Examining Figure 15(b) shows that the actual angular velocity is different than the required one by 0.05 rad/s. This figure also shows that the angular separation of 120 deg is kept during the experiment. Figure 15(a) shows that the robots keep moving in a distance of 1.3 m from the center point. Another experiment was conducted in a similar manner to confirm the results (see Figure 16). This experiment included a more rapid rotation with angular velocity $\omega = 0.071$ rad/s.

Collision avoidance The third experiment examined collision avoidance. In this experiment the three robots attempt to reach their target positions while a 4th robot moves as an obstacle. Whereas the 3 robots operate autonomously the 4th robot is controlled by a human operator. At the first 30 s (see Figure 17(c), solid lines) the robots move to their target positions on a circle with a radius of 0.7 m. At the same time the obstacle is still out of the sphere of influence of the other robots. In the next step (see Figure 17(c), dashed lines) the obstacle robot moves next to robot 1 and then next to robot 2. Both robots avoid the obstacle by moving away from the their target positions. This behavior can be observed also in Figure 17(b). Notice the change in the trajectories of robot 1 (after 30 s) and robot 2 (after 35 s). Although the obstacle is not moving next to robot 0, the motion of the other robots affects the trajectory. When the obstacle robot moves away, the formation resumes its

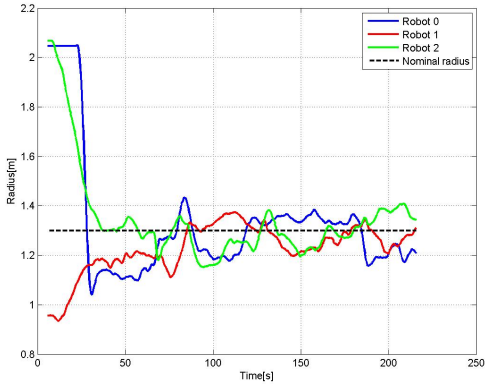

(a) Radius

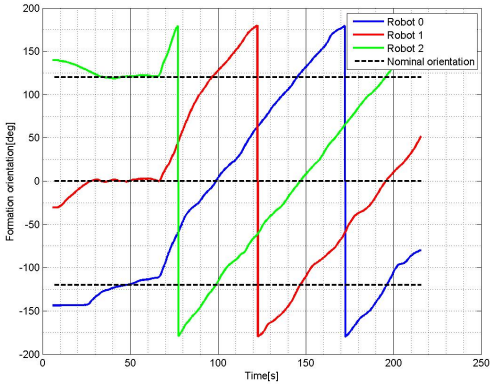

(b) Angular separation

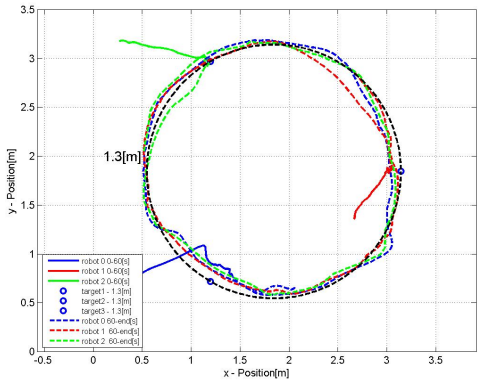

(c) Trajectory

Figure 15. Acquisition of a rotating formation - experiment 1

original trajectory. As seen before, the reconfiguration is rather fast and takes about 30 s.

Discussion of Results in both Facilities

The experiments in both facilities (TEAMS and DSSL) showed that the guidance based on the artificial potential is working and can be transferred into a different environment without too much effort.

Table 2 shows the most important parameter for both facilities, needed to understand the differences. Comparing the experiments on TEAMS and DSSL the following can be concluded:

- Formation acquisition, formation keeping as well as formation re-acquisition worked in both facilities as it can be seen in figures 10 and 13.
- The collision avoidance performed also within expectation as shown in figures 12 and 17.
- The dynamic response of the vehicles on the change of set points is not unexpected different in both facilities. As it can be seen in figure 10 the formation acquisition takes a time in

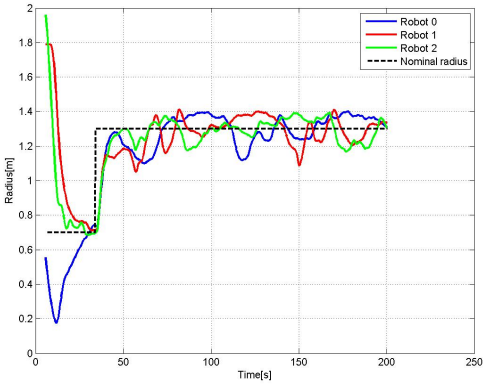

(a) Radius

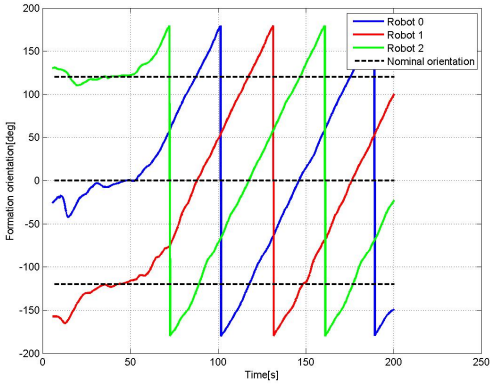

(b) Angular separation

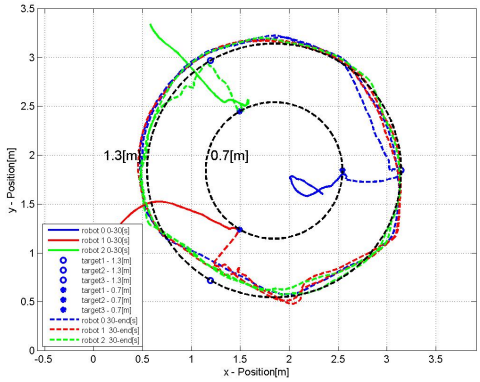

(c) Trajectory

Figure 16. Acquisition of a rotating formation - experiment 2

	TEAMS	DSSL
Max. acceleration $[mm/s^2]$	2.8	180
Max. design velocity $[m/s]$	0.07	0.54
k_a, k_d $[m^2]$	0.25	0.4
b $[s^{-1}]$	1.2	4
d $[s^{-1}]$	0.1	1
Tracking error $[mm]$	<2	??
Thruster actuation	Proportional	PWM
Control error $[m]$	0.05	0.12

Table 2. Parameter comparison of both test facilities

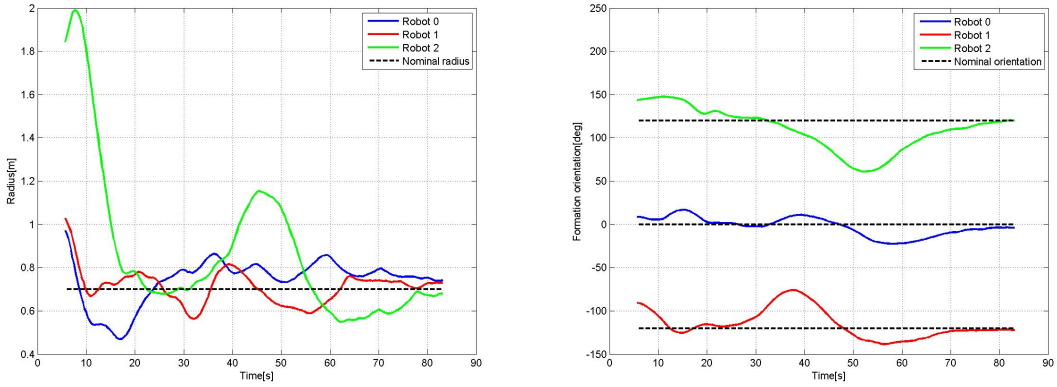

(a) Radius

(b) Angular separation

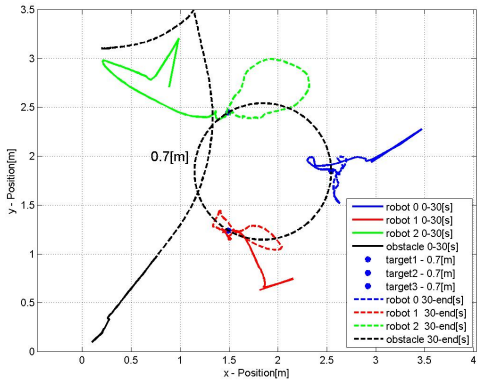

(c) Trajectory

Figure 17. Collision avoidance

the order of about 100 s. The step response at DSSL took less than 10 s shown in figures 13 and 14. This is the effect of the different dynamic properties of the vehicles, mainly maximum acceleration, but more of the dominating time constant $1/d$ while docking to a target position in the two different setups. In TEAMS the maximum acceleration is 2.8 mm/s^2, while the dominating time constant is 10 s (see table 2). The DSSL vehicles have a maximum acceleration of 180 mm/s^2 and a dominating time constant of 1 s, which is 10 times faster than for the TEAMS configuration. Thus the time for the formation acquisition for DSSL is also 10 times smaller than for the TEAMS vehicles.

- The control accuracy of when keeping the positions in the formation is again different in both facilities. In TEAMS the position control error is in the order of 0.05 m as shown in figure 11. At the DSSL it is about 0.12 m (see table 2). This difference is again a consequence of the different setups. The deviation comes from different factors like sensor accuracy, actuation noise and actuator quantization. The main difference is probably the fact that the vehicles on TEAMS have proportional thrusters while the vehicles at DSSL have pulsed actuators.

In summary, the results show the applicability of the artificial potential for formation applica-

tions. With the implementation and experiments on two different facilities in addition to previous simulations[3] experiences were gathered which can be summarized in the following lessons learned:

- The similar results of the same algorithm on both testbeds verify the applicability of the two testbeds as reference for formation flying missions.
- Errors in sensors and actuators has to be taken into account to interpret the results.

CONCLUSIONS

In this paper we presented the implementation of an autonomous and distributed path-planning method for satellite formations and swarms. The method is based on the definition of a virtual kinematical field from generic behaviors like *Gather*, *Avoid* and *Dock*. In addition a control algorithm is needed to make each satellite follow the defined kinematical field autonomously. This gives us the possibility to do formation acquisition, reconfiguration and reorientation while avoiding collision with other satellites.

The method has been implemented and tested on two test setups which are based on air cushion vehicles (TEAMS and DSSL). Formation acquisition and reconfiguration have been shown in these environments as well as the capability of the method to do collision avoidance in case of an abnormal behavior of one satellite. The guidance algorithm worked well in both facilities. Due to the difference of the two setups the results in terms of achieved speed and control accuracy are - of course - different. However, the results show that the guidance algorithm can be easily adapted to a different environment producing comparable results.

ACKNOWLEDGMENTS

This research was supported by the German-Israeli Foundation under Grant 1180-220.10.

REFERENCES

[1] Izzo, D. and Pettazzi, L. "Autonomous and Distributed Motion Planning for Satellite Swarm." Journal of Guidance, Control, and Dynamics, Vol. 30, No. 2, pp. 449–459, March-April 2007.

[2] Schlotterer, M. and Novoschilov, S. "On-Ground Path Planning Experiments for Multiple Satellites." "23rd International Symposium on Space Flight Dynamics 2012," Oktober 2012.

[3] Novoschilov, S. Pfadplanung und Kollisionsvermeidung für Satellitenformationen und -schwärme. Master's thesis, RWTH Aachen, 2012.

[4] Schlotterer, M. and Theil, S. "Testbed for On-Orbit Servicing and Formation Flying Dynamics Emulation." AIAA, editor, "AIAA Guidance, Navigation and Control Conference and Exhibit," AIAA-2010-8108. 2010.

[5] Li, S., Cui, P., and Cui, H. "Autonomous navigation and guidance for landing on asteroids." Aerospace Science and Technology, Vol. 10, No. 3, pp. 239–247, 2006.

[6] McClelland, R. S. "Spacecraft Attitude Control System Performance Using Pulse-Width Pulse-Frequency Modulated Thrusters." Tech. rep., DTIC Document, 1994.

[7] Song, G., Buck, N. V., and Agrawal, B. N. "Spacecraft vibration reduction using pulse-width pulse-frequency modulated input shaper." Journal of Guidance, Control, and Dynamics, Vol. 22, No. 3, pp. 433–440, 1999.

[8] Ayre, M., Izzo, D., and Pettazzi, L. "Self Assembly in Space Using Behaviour Based Intelligent Components." "TAROS, Towards Autonomous Robotic Systems," 2005.

[9] Regher, M. W., Acikmese, A. B., Ahmed, A., Aung, M., Bailey, R., Bushnell, C., Clark, K. C., Hicke, A., Lytle, B., MacNeal, P., Rasmussen, R. E., Shields, J., and Singh, G. "The Formation Control Testbed." "IEEE Aerospace Conference Proceedings," 2004.